Journal of Peptide Science
J. Pept. Sci. 2006; **12**: 550–558
Published online 30 May 2006 in Wiley InterScience (www.interscience.wiley.com). DOI: 10.1002/psc.764

JOURNAL OF PEPTIDE SCIENCE

Synthesis and conformational analysis of Id2 protein fragments: impact of chain length and point mutations on the structural HLH motif

NOEMI COLOMBO and CHIARA CABRELE*
Fakultät für Chemie und Pharmazie, Universität Regensburg, Universitätsstraße 31, 93053 Regensburg, Germany

Received 8 December 2005; *Revised 20 February 2006*; *Accepted 24 March 2006*

Abstract: The Id proteins are negative regulators of several basic-helix-loop-helix (HLH) transcription factors, including the ubiquitous E factors and the tissue-specific myogenin-regulating factors. Id1 through Id4 contain highly identical HLH domains but different *N*- and *C*-terminal extensions. Beside the heterodimerization with the parent HLH factors, Id2 was shown to additionally interact with the retinoblastoma protein and to be overexpressed in neuroblastoma. Thus, Id2 represents an interesting target for cancer therapy based on the inhibition of protein–protein interactions. Here we present the synthesis and circular dichroism (CD) analysis of peptides derived from point mutations and *N*-/*C*-terminal truncations of Id2. The helix character of the HLH domain (residues 36–76) was reduced upon substitution of Met39/-62 and Cys42 with Nle and Ser, respectively, suggesting a structural role of these side chains. The largest sequence that could be obtained by stepwise solid-phase peptide synthesis (SPPS) with Fmoc strategy spanned the entire HLH motif (with Cys42 replaced by Ser) and part of the *C*-terminus (residues 77–110). This 75-residue long fragment was less helical than the isolated HLH domain and had propensity to aggregate, which was correlated with the presence of the flanking residues *C*-terminal to helix-2. By CD analysis of an equimolar mixture of the sequence 36–110 with the *N*-terminus 1–35, noncovalent interactions between the two peptides were detected, which, however, changed upon aging. In contrast, the mixture of the HLH sequence 36–76 with the *N*-terminus was characterized by a stabilized helix structure that was maintained also upon aging. Presumably, the *N*-terminal region interacted with the folded HLH motif in a specific manner, whereas only unspecific, weak contacts occurred with the partly unfolded HLH domain and/or the immediate flanking residues 77–110. Copyright © 2006 European Peptide Society and John Wiley & Sons, Ltd.

Keywords: Id proteins; helix loop helix; solid-phase synthesis; circular dichroism

INTRODUCTION

The Id proteins (Id1-4) are helix-loop-helix (HLH) transcription factors with no DNA-binding function [1,2], as they do not possess a basic region *N*-terminal to the HLH motif, which is instead present in the related basic-HLH proteins [3]. The 41-residue long HLH domain is highly conserved within the Id family, whereas the *N*- and *C*-termini are different both in amino acid composition and length. The HLH sequence is essential for the interaction of the Id proteins with several basic-HLH factors, leading to the formation of heterodimers unable to bind DNA. Thus, the Id proteins inhibit the DNA transcription mediated by basic-HLH factors [4], including the ubiquitously expressed E proteins and the tissue-specific myogenin-regulating factors (e.g. MyoD).

With the exception of Id1, the other Id proteins contain a conserved *N*-terminal phosphorylation site (Ser-Pro-Val-Arg), which has been shown to play a role in regulating the inhibitory activity of the Id proteins. On the one hand, phosphorylated Id2 and Id3 could not prevent the formation of DNA-basic-HLH complexes [5,6]; on the other hand, phosphorylation of Id2 was required for vascular smooth cell proliferation [7].

Beside Ser phosphorylation, protein degradation is another mechanism that regulates the Id function; in the case of Id2, ubiquitination has been proposed to occur via molecular recognition of its *N*-terminal tail, possibly by the ubiquitin ligase E3 [8], whereas ubiquitination of Id1 and Id3 is mediated by the COP9 signalosome [9].

The Id proteins play a crucial role during development and are widely expressed in fetal tissues, while being downregulated in healthy adult tissues. In general, they inhibit differentiation and promote proliferation [10–12]. A role of the Id proteins in tumorigenesis has also been established; indeed, overexpression of the Id genes was found in several cancer types, including breast, colorectal, astrocytic and pancreatic cancer [13,14]. In glial tumors the expression level of the Id proteins correlated with the degree of malignancy [15]. There is evidence that the proto-oncogenic properties of the Id proteins are based on the antagonism not only of basic-HLH factors, but also of the retinoblastoma protein (pRb). Indeed, when present in molar excess, Id2 inactivates the pRb pathway directly by binding

*Correspondence to: C. Cabrele, Fakultät für Chemie und Pharmazie, Universität Regensburg, Universitätsstraße 31, 93053 Regensburg, Germany; e-mail: chiara.cabrele@chemie.uni-regensburg.de

to the hypophosphorylated pRb [16,17]. Indirectly, Id1 blocks the pRb-controlled tumor suppression by inhibiting the Ets-mediated transcription of $p16^{INK4A}$ [18]. Thus, due to its implication in tumorigenesis, the Id family represents an important target in cancer therapy and diagnostics, and artificial Id antagonists would be useful tools against tumor growth [19].

Among the Id proteins, Id2 has attracted much interest because of its ability to bind to pRb and related proteins, and because of the fact that it might be a target of the proto-oncogen *N-myc*, whose amplification and overexpression are a hallmark of neuroblastoma [20]. In addition, the *N*-terminus of Id2, but not its HLH motif, was found to induce apoptosis by increasing the expression of the proapoptotic *BAX* gene [21]. As the protein–protein interaction profile of Id2 is unique within its family, we are interested in its conformation. First, we investigated the possibility to obtain large Id2 fragments by standard solid-phase peptide synthesis (SPPS). The sequence 36–110 was the largest one that could be assembled by stepwise SPPS in combination with the 9-fluorenylmethoxycarbonyl (Fmoc) strategy. Unfortunately, fragments containing the complete *C*-terminal region (residues 77–134) turned out to be poorly accessible with this chemical approach, which should be attributable to strong peptide chain aggregation during elongation.

The secondary structure of the synthetic Id2 analogs was analyzed by circular dichroism (CD) spectroscopy. Noteworthy, all fragments containing the *C*-terminal sequence 77–110 showed low solubility and/or high tendency to aggregate. Even the usually highly stable Id2 HLH motif was negatively affected by the *C*-terminal elongation of helix-2, suggesting that this flanking region could modulate the folding and stability of the adjacent domain.

MATERIALS AND METHODS

Chemicals

The N^{α}-Fmoc protected amino acids were purchased by MultiSynTech (Witten, Germany) and Novabiochem (Merck Biosciences GmbH, Schwalbach/Ts., Germany). Rink amide 4-methylbenzhydrylamine (MBHA) resin and HBTU were from MultiSynTech. Wang resin was from Novabiochem. HOBt, DIPEA, TFA, triisopropylsilane (TIS), trimethylsilylbromide (TMSBr), α-cyano-4-hydroxycinnamic acid and sinapinic acid were from Fluka (Taufkirchen, Germany). The following peptide-synthesis-grade reagents were purchased by Biosolve (Valkenswaard, The Netherlands): piperidine, 1-methyl-2-pyrrolidinone (NMP), DMF and diethylether. HPLC-grade acetonitrile (ACN) and TFA for UV spectroscopy were from Biosolve. *N*, *N*′-diisopropylcarbodiimide (DIC) was from Acros (Geel, Belgium). Sodium hydrogenphosphate and dihydrogenphosphate, acetic anhydride, acetic acid and 1,2-ethanedithiol (EDT) were obtained from Merck (Darmstadt, Germany).

Peptide Synthesis

All peptides were prepared on a 0.018 mmol scale by solid-phase methodology using the automatic synthesizer *Syro-I* (MultiSynTech). Double couplings (2×40 min) were performed with N^{α}-Fmoc-amino acids (5 equiv) activated *in situ* with HBTU (5 equiv), HOBt (5 equiv) and DIPEA (10 equiv). Fmoc cleavage was accomplished by treating the peptidyl resin with 40% piperidine in DMF/NMP (80 : 20 v/v) for 3 min, followed by a second treatment with 20% piperidine for 10 min. *N*-terminally truncated Id2 analogs were acetylated at the *N*-terminus by acetic anhydride (10 equiv) and DIPEA (10 equiv) in DMF for 20 min. *C*-terminally truncated Id2 analogs were synthesized as *C*-terminally amidated peptides using the Rink amide MBHA resin (loading: 0.6 mmol/g). The Id2 segments containing the entire *C*-terminus were prepared starting from the Wang resin (loading: 1.0 mmol/g), which was first manually preloaded using Fmoc-Gly-OH (5 equiv), HOBt (5 equiv), DIC (5 equiv) and DIPEA (5 equiv). The new loading was 0.7 mmol/g, as determined by the UV absorption of the fluorenylmethyl-piperidine adduct at 300 nm. The remaining free hydroxybenzyl groups were then acetylated. The peptides were cleaved from the resin and simultaneously deprotected with the mixtures TFA/water/TIS (90 : 5 : 5 v/v) or TFA/water/TIS/EDT (90 : 3 : 4 : 3 v/v) for 2.5 h. The crude peptides were precipitated from ice-cold diethyl ether and recovered by centrifugation at 3 °C for 8 min. Several ether washes/centrifugation cycles were carried out to efficiently remove the scavengers.

Peptide Purification and Characterization

The crude products were dissolved in 30% acetic acid and purified by RP-HPLC using an Agilent equipment and a Luna C-18(2) column from Phenomenex (10 μm, 250×21.2 mm). The binary elution system was (A) 0.004% (v/v) TFA in water and (B) ACN. The gradient was 10–70% B over 40 min, with a flow rate of 21 ml/min. UV detection was made at 220 nm. Analytical RP-HPLC was performed on the following equipment: L-6200A intelligent pump from Merck, HP detector Series 1050 from Agilent, and Luna C-18(2) column from Phenomenex (90 Å, 3 μm, 150×4.60 mm). The binary elution system was (A) 0.012% (v/v) TFA in water and (B) 0.01% (v/v) TFA in ACN. The gradient was 10–70% B over 40 min, with a flow rate of 1 ml/min. UV detection was made at 220 nm. The mass spectra were recorded on a Future GSG spectrometer (Bruchsal, Germany) for MALDI-TOF analysis, and on a ThermoQuest spectrometer (Finnigan) for LC-ESI analysis.

CD Spectroscopy

The CD spectra were recorded on a JASCO J710 spectropolarimeter, using a quartz cell with a path length of 0.02 cm. Peptide stock solutions were prepared in phosphate buffer (100 mM, pH 7.3), and their concentration was determined by measuring the UV absorbance of the Tyr residues at 280 nm ($\varepsilon = 1480\ M^{-1}\ cm^{-1}$) [22]. In the case of peptides lacking any chromophore, a stock solution was prepared assuming a peptide content of 70%. The stock solution of peptide **3** was prepared in methanol. For each CD spectrum ten scans were accumulated using the following parameters: 1 nm step resolution and bandwidth, 2 s response time, 20 nm/min scan

speed and 20 mdeg sensitivity. The CD spectrum of the buffer was subtracted from that of the peptide to eliminate interferences from the cell, solvent and optical equipment. Noise reduction was obtained by a Fourier transform filter with the program Origin (OriginLab Corporation, Northampton, MA, USA). The secondary structure element composition was extrapolated by submitting the experimental CD spectra to the Dichroweb on-line server [23]. The algorithm Contin [24] provided the best fitting in all cases.

RESULTS AND DISCUSSION

Solid-phase Synthesis of Id2-related Peptides

The C-terminal fragments. The *C*-terminal domain of Id2 (product **1**, Table 1) consists of 58 residues, including a considerable number of the β-branched Leu (8) and Ile (4), as well as of Ser (9), Thr (5), Asx (6) and Glx (6). Peptide chain assembly starting from the *C*-end, Gly134, using Fmoc chemistry and standard solid-phase procedures led to a crude peptide with very low homogeneity (Figure 1(a)), which prevented any attempt of purification. Instead, the shorter fragment 99–134 (**2**) was obtained as the major product (Figure 1(b)) and was then efficiently purified by preparative RP-HPLC. This suggests that the synthetic problems encountered in the preparation of the fragment 77–134 occurred during elongation from residue 98 to residue 77. However, the fact that the sequence 77–124 (**3**) was obtained with good homogeneity (Figure 1(c)) indicated that the difficulty of peptide chain assembly was dependent on the starting position. Indeed, when Glu119 was chosen as the *C*-terminal residue, even after only 16 couplings a complex mixture of products was cleaved from the resin (product **4**, Table 1 and Figure 1(d)), which could not be further identified by mass spectrometry. The different accessibility of the last two Id2 fragments presumably reflected different aggregation propensity of the peptide chains; in fact, starting from Leu124 rather than from Glu119 was probably advantageous because the Pro residue located four positions apart from the *C*-end, Pro121, might have induced a backbone bending, thus reducing the aggregation of the growing sequence that was predicted to form preferentially β-sheets in the region 103–115 on the base of the Chou and Fasman analysis [25]. It has been recently reported that solid-phase synthesis of peptides forming aggregates [26] could be improved by using the pseudoproline dipeptides developed by Mutter and coworkers [27]. As segment **4** was suitable for the pseudoproline chemistry because of the presence of several Thr and Ser residues, the synthesis was repeated by introducing the pseudoproline at positions 111 and 114. However, also this approach led to a poorly homogeneous product.

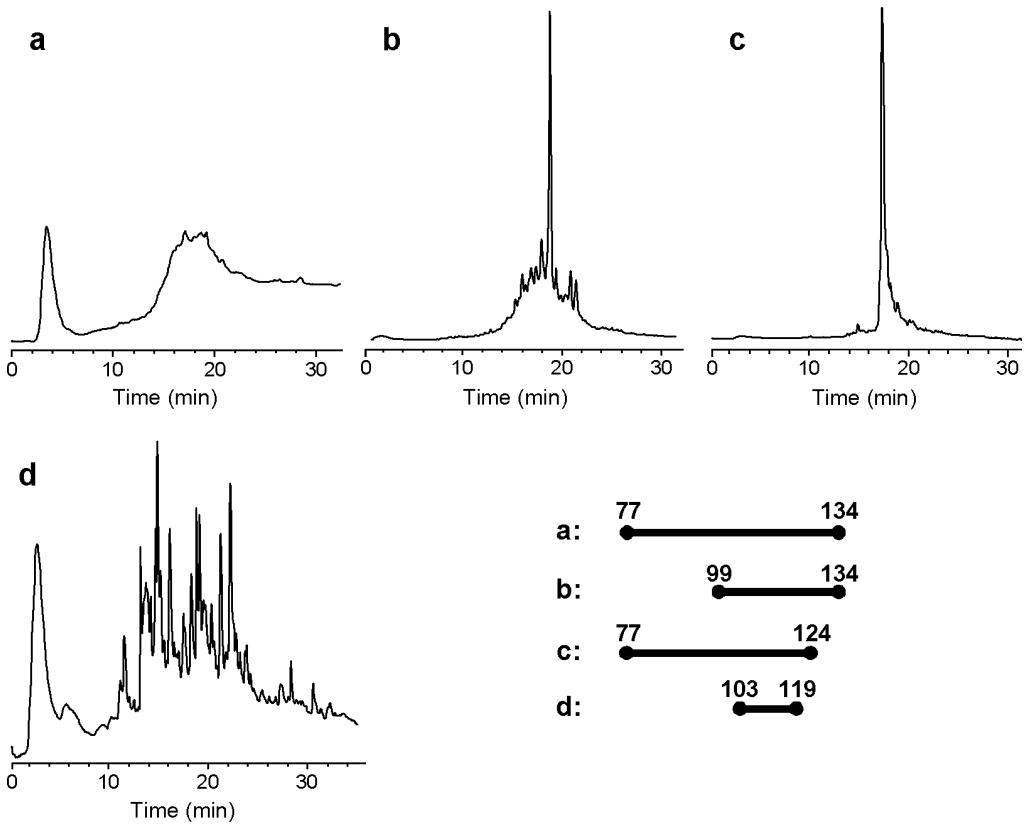

Figure 1 HPLC profiles of the crude peptides **1**–**4**: (a–d) *Ac*-(77–134)-*OH*, *H*-(99–134)-*OH*, *Ac*-(77–124)-NH_2 and *Ac*-(103–119)-NH_2.

Table 1 Amino acid sequence of the human Id2 protein and analytical data of the synthetic Id2 fragments

Human Id2[a]

M[1]KAFSPVRSVRKNSLSDHSLGISRSKTPVDDPMSL[35]LYNMND-CYSKLKELVP[51]SIPQNKKVS[60]KMEILQHVIDYILDLQ[76]-IALDSHPTIVSLHHQRPGQNQASRTPL-TTLNTDISILSLQASEFPSELMSNDSKALCG[134]

Synthetic Id2 polypeptides

Product number	Chain length	MW_{calcd} (Da)	MW_{found} (Da)	t_R (min)
1	77–134[b]	6285.09	n.d.[e]	n.d.[e]
2	99–134	3912.44	3915	29.0
3	77–124[b,c]	5276.94	5278	28.0
4	103–119[b,c]	1860.11	n.d.[e]	n.d.[e]
5	61–110[b,c]	5727.59	5729	21.5
6	51–110[b,c]	6806.87	6807.8[d]	19.0
7	[S^{42}]-(36–110)[b,c]	8605.96	8605.5[d]	19.5
8	60–76[b,c]	2099.50	2100	21.5
9	36–52[b,c]	2058.42	2060	18.7
10	36–76[b,c]	4906.85	4907.7[d]	20.5
10a	[$Q^{38,40}$, E^{41}]-(36–76)[b,c]	4948.93	4949.7[d]	21.5
10b	[$Nle^{39,62}$, S^{42}]-(36–76)[b,c]	4854.71	4857	19.0
11	1–35[c]	3843.48	3845	10.8

[a] Underlined sequences: helix-1 (36-51), loop (52-60) and helix-2 (61-76).
[b] The fragment is *N*-terminally acetylated.
[c] The fragment is *C*-terminally amidated.
[d] Determined by LC-ESI-MS (all others were determined by MALDI-TOF-MS).
[e] Not determined.

Although synthetically accessible, the Id2 sequence starting from Leu124 was found to be only moderately soluble both in water and phosphate buffer, whereas it could be dissolved in methanol and in mixtures of methanol/water.

A good starting point for the synthesis of *C*-terminally truncated Id2 analogs was Ile110, as shown by the HPLC profiles of the crude products of peptides **5**–**7** (Figure 2). For the synthesis of **7** that contained the complete HLH motif with one mutation at position 42 (Cys was replaced with Ser), the pseudoproline dipeptide Asp(O*t*Bu)-Ser($\Psi^{Me,Me}$pro) was coupled instead of the single amino acids Asp41 and Ser42, to reduce the risk of chain aggregation during elongation [27].

The HLH motif. To investigate the intrinsic conformation of the two helices forming the HLH structural motif of Id2, the sequences 36–52 and 60–76 reproducing helix-1 and helix-2, respectively, were synthesized. Helix-1 (**9**) showed a major degree of difficulty in the chain assembly relative to helix-2 (**8**), as deduced by the different homogeneity of the corresponding crude products (Figure 3(a–b)). Also during the synthesis of

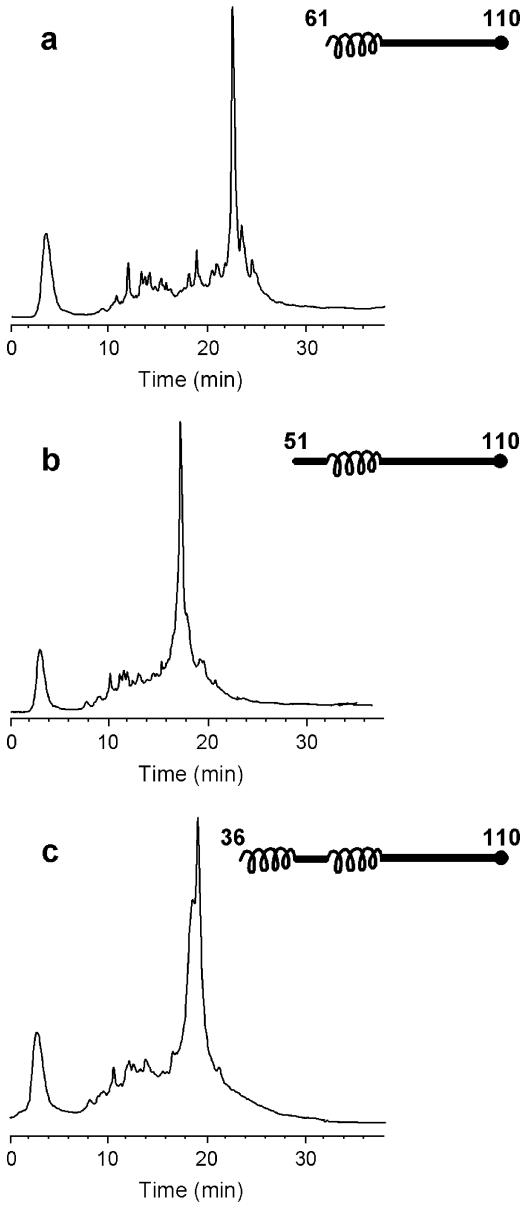

Figure 2 HPLC profiles of the crude peptides **5**–**7**: (a–c) *Ac*-(61–110)-NH_2, *Ac*-(51–110)-NH_2 and *Ac*-[S^{42}]-(36–110)-NH_2.

the entire HLH motif (**10**) a consistent amount of by-products was produced, which accumulated mostly in the region of helix-1 (Figure 3(c)). LC-ESI-MS analysis indicated the presence of the truncated sequences 43–76 and 42–76, and of the sequence lacking Cys42. When the last couplings were carried out manually and monitored by the ninhydrin test [28], it was observed that especially Asp41, Met39 and Tyr37 were difficult to be acylated. Longer coupling reactions and introduction of a capping step, however, did not lead to a significant improvement of the quality of the crude product. To exclude the formation of aspartimide that could eventually lead not only to the β-isomer but also to the breakage of the backbone, Asn38, Asn40 and Asp41 were substituted by Gln and Glu (**10a**).

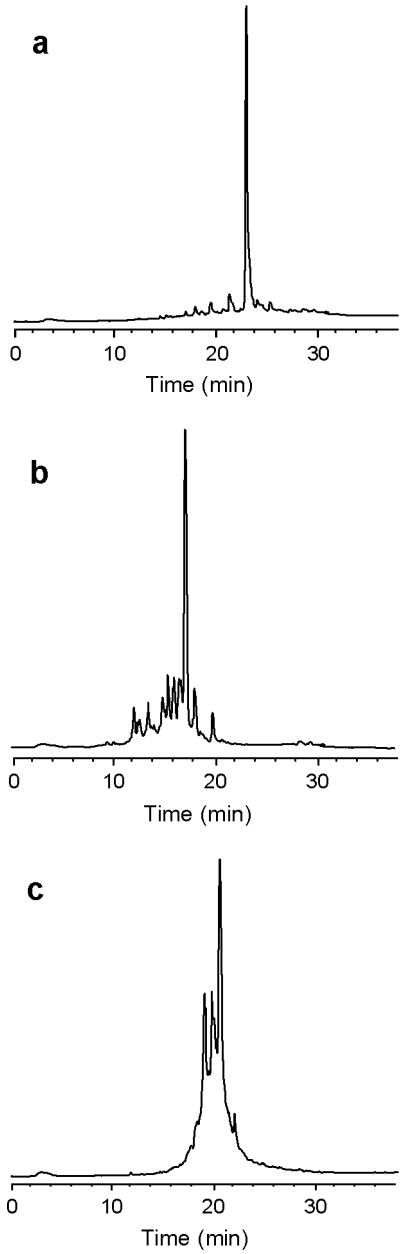

Figure 3 HPLC profiles of the crude products of: (a) helix-2 (**8**), (b) helix-1 (**9**) and (c) the native HLH motif (**10**).

However, as the HPLC profiles of the crude peptides **10** and **10a** were almost superimposable, it was concluded that the aspartimide formation, if ever occurred, was a minor event. In contrast, a consistent by-product of the synthesis of the HLH motif was its Met-oxidized species (+16 Da), which resulted to be resistant against reduction with TMSBr/EDT/TFA. Peptide **10b** containing the replacements Nle → Met39/-62 and Ser → Cys42 was prepared to have a HLH analog insensitive to oxidative processes and thus easier to handle, but it was obviously still contaminated by the same truncated and deleted sequences found for the native HLH peptide.

CD Spectroscopy

Peptides containing the Id2 C-terminal region. The CD spectrum of the Id2 *C*-terminal segment 101–134 in phosphate buffer (100 mM, pH 7.3) was previously reported [29] and resembled that of a random coil. Unfortunately, in the present work the synthesis of the full-length *C*-terminus 77–134 by stepwise solid-phase methodology and Fmoc chemistry was not successful, but it was possible to obtain the analog spanning residues 77–124. Because of the very low solubility both in water and in phosphate buffer, the CD spectra of **3** were recorded in methanol and methanol/water mixtures at a peptide concentration of 50 μM (Figure 4). A low-intensity, α-helix-like curve was recorded in methanol, which was characterized by two negative bands at 223 nm (amide $n-\pi^*$ transition) and 209 nm (amide $\pi-\pi^*$ transition), and by a positive band near 190 nm with a crossover at 200 nm. The ratio R between the ellipticity values at 223 and 209 nm was 0.75. Despite the helix-like shape, this spectrum is remarkably less intense than it is expected for a α-helix, which is probably due to peptide aggregation. Upon water addition, the CD intensity further decreased, and at water percentage ≥60% the shape changed from helix-like to random-like, showing a negative Cotton effect close to 200 nm. The absence of an isodichroic point suggests that it was not a two-state transition.

Unlike peptide **3**, peptides **5**–**7** were soluble in phosphate buffer (100 mM, pH 7.3), in which they were dissolved at the concentration of 30 μM for CD analysis. The spectra showed two negative bands at 222 nm (amide $n-\pi^*$ transition) and 204 nm (amide $\pi-\pi^*$ transition) and a positive one near 190 nm, with a crossover at 195–197 nm (Figure 5). Secondary structure element composition was estimated by using the algorithm Contin [24] (Table 2), which indicated the presence of similar amounts of α-helix and β-sheet structures (the α/β ratios were ~1 for **5** and **7**, and 0.6 for **6**). This suggests that these peptides were prone to

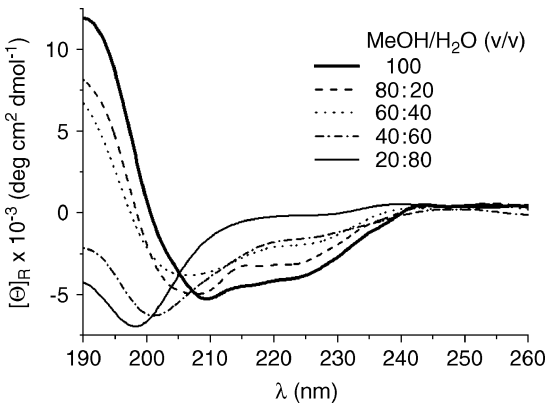

Figure 4 CD spectra of *Ac*-(77–124)-NH_2 (**3**) at the concentration of 50 μM in methanol/water (the ratios of the two solvents are reported in the figure).

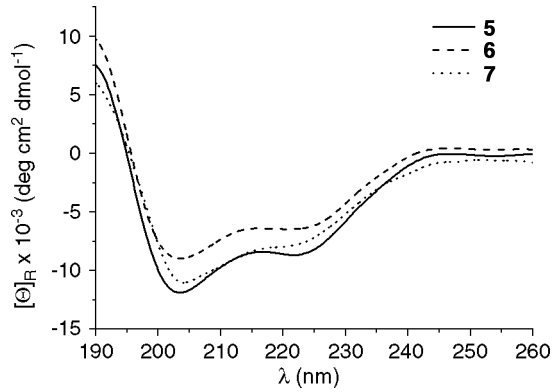

Figure 5 CD spectra of *Ac*-(61–110)-NH_2 (**5**), *Ac*-(51–110)-NH_2 (**6**) and *Ac*-[S^{42}]-(36–110)-NH_2 (**7**) at the concentration of 30 μM in phosphate buffer (100 mM, pH 7.3).

aggregate, which was also supported by the observation that the CD spectra recorded at the concentrations of 30 and 100 μM were characterized by different intensities (the more concentrated sample gave a less intense CD signal). The conformation of peptides **5**–**7** was not only concentration-dependent, but also time-dependent; indeed, aging of **5** and **6** favored the α-helix at the expense of the β-sheet structure, whereas aging of **7** increased the β-sheet structure at the expense of the α-helix.

The weak helix character of the Id2 fragments **5** and **6** is not very surprising, as they contain only part of the HLH fold (helix-2 with or without the loop); instead, it was surprising to see that peptide **7**, although spanning the complete HLH motif, was not able to adopt a stable helix conformation. Of course, modification of helix-1 by replacing Cys42 with Ser might have affected the stability of the HLH fold; however, this cannot explain the aggregation propensity that was observed not only for peptide **7**, but also for peptides **5** and **6** that lack helix-1. In contrast, as all three peptides shared the flanking residues *C*-terminal to helix-2, which were also present in the poorly soluble and aggregation-prone peptide **3**, it is likely that the common tendency of these four Id2 fragments to aggregate arise from such region.

Table 2 Conformational properties of the synthetic Id2 fragments

Product number	Number of residues	*R* value[a]	Secondary structure element by Contin (%)[b]			
			Helix (number of residues)	β Sheet	Turns	Un-ordered
5	50	0.7	23(12)	20	23	34
6	60	0.72	16(10)	27	21	36
7	75	0.71	21(16)	23	24	32
8	17	0.87	61(10)	6	1	32
9	17	0.3	0	6	10	84
10	41	1.03	86(35)	0	8	6
10b	41	0.96	48(20)	9	21	22

[a] The *R* value is defined as the ratio between the CD intensities of the amide $n-\pi^*$ and $\pi-\pi^*$ bands.
[b] The CD spectra were analyzed by using the on-line server Dichroweb [23].

Peptides related to the Id2 HLH motif. The Id2 HLH motif 36–76 has been previously investigated by CD spectroscopy in phosphate buffer (100 mM, pH 7.3), and it has been shown to adopt a helical conformation that is stable also in the presence of high concentrations of guanidine hydrochloride (up to 4 M) [29]. Moreover, the CD spectrum was characterized by an *R* value >1. In this work the Id2 HLH analog **10b** was prepared by replacing the sulfur-containing residues Met and Cys with Nle and Ser, respectively. These substitutions have the advantage to avoid problems related with peptide

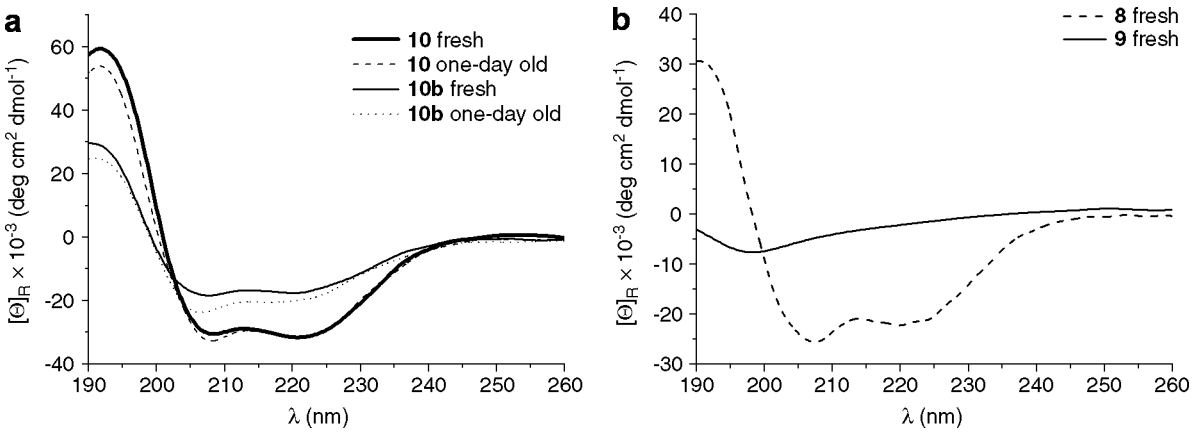

Figure 6 (a) CD spectra of *Ac*-(36–76)-NH_2 (**10**) and *Ac*-[$Nle^{39,62}$,S^{42}]-(36–76)-NH_2 (**10b**) at the concentration of 30 μM in phosphate buffer (100 mM, pH 7.3). (b) CD spectra of helix-2 (**8**) and helix-1 (**9**) at the concentration of 220 and 180 μM, respectively, in phosphate buffer.

oxidation; moreover, as they are highly conservative, no significant conformational changes are expected. Instead, the CD spectrum of the three-point mutated HLH sequence was found to be less intense than that of the native motif, and the amide $\pi-\pi^*$ band was slightly blue-shifted. In addition, the *R* value became <1. Based on the CD data reported in Figure 6(a), helical contents of 86% for the native and of 48% for the mutated HLH peptide were estimated with the algorithm Contin [24]. These results suggest that the Cys and/or Met side chains are important for the HLH fold, and even subtle substitutions are badly tolerated. Thus, peptide **10b** is not a suitable candidate to be used in place of the native sequence for further conformational analyses. However, an NMR study of this analog and of the unmodified sequence would be interesting to identify the structural differences induced by amino acid replacement.

In contrast to the one-point mutated HLH sequence conjugated to the Id2 *C*-terminal region **7**, the isolated HLH motifs of peptides **10** and **10b** were found to be stable upon aging, with only a moderate increase in the intensity of the CD band corresponding to the amide $\pi-\pi^*$ transition (Figure 6(a)). This observation again underlines the negative impact of the *C*-terminal extension on the folding and stability of the adjacent HLH region.

Peptides reproducing helix-1 and helix-2. The two helices forming the Id2 HLH motif showed two different CD profiles in phosphate buffer, which indicated the presence of unordered structure for helix-1 and of helical conformation for helix-2 (Figure 6(b)). This suggests that the intrinsic helix propensity of helix-2 was much higher than that of helix-1. However, the conformational stability of helix-2 was concentration-dependent, which can be explained with the tendency of single amphipathic helices to interact with each other through their hydrophobic faces.

Noncovalent interactions between the Id2 N-terminus and the HLH-containing peptides. The Id2 *N*-terminal fragment 1–35 (**11**) has been shown to adopt an unordered conformation in phosphate buffer [29]. However, when it was mixed with the native HLH motif (**10**) in a 1 : 1 ratio, the CD spectrum was characteristic of a α-helix and the intensity of the two minima at 222 and 206 nm was higher than the arithmetic sum of the intensities of the two separated fragments (Figure 7(a)). This indicates that an interaction of the *N*-terminus with the HLH fold could be detected, which apparently led to helix stabilization in the complex and was maintained also upon aging.

When the experiment described above was carried out using the segment 36–110 (**7**) instead of the HLH motif (**10**), the CD spectrum of the mixture was less intense than the sum of the spectra of the two separated fragments (Figure 7(b)), suggesting an increase in β-structure at the expense of α-helix upon mixing.

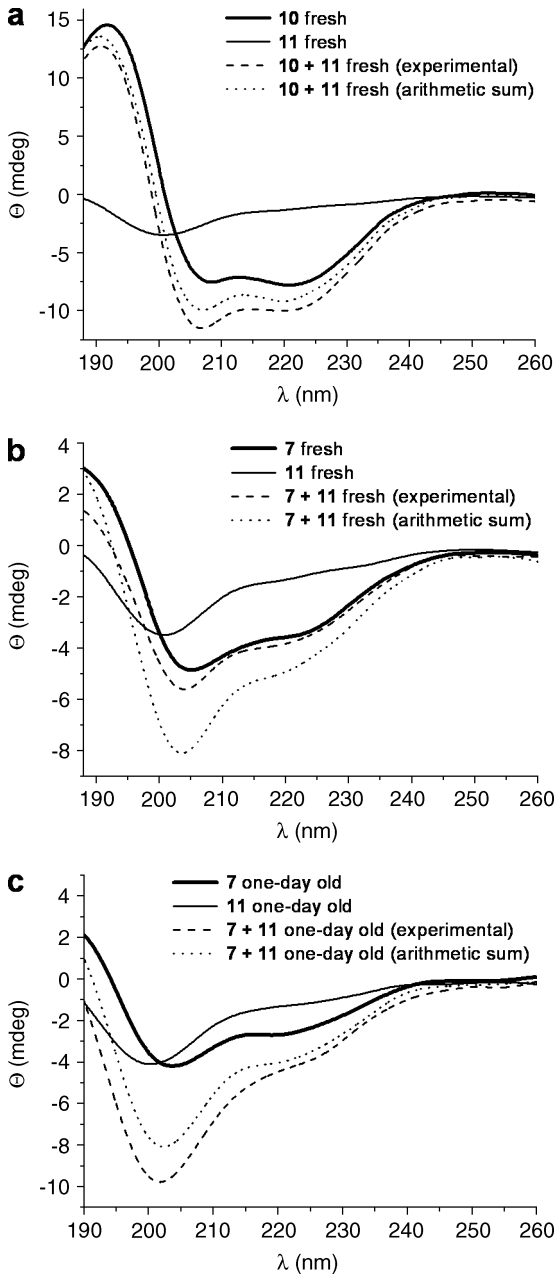

Figure 7 CD spectra of equimolar mixtures of the *N*-terminal sequence 1–35 (**11**) with (a) the native HLH motif *Ac*-(36–76)-NH_2 (**10**) and (b and c) the fragment *Ac*-[S^{42}]-(36–110)-NH_2 (**7**). Each component in the mixture was at the concentration of 30 μM. The CD spectra of the individual peptides (30 μM each) and their arithmetic sum are also shown.

However, such changes seemed to be reversible, as the CD spectrum of the 1-day-old mixture gained intensity and was close to the sum of the CD spectra of the two individual components (Figure 7(c)). Presumably, the increased tendency of peptide **7** to self-aggregate became predominant, thus reducing the possibility of interaction with the *N*-terminus. The different effect of the *N*-terminus on the HLH motif alone and conjugated to the *C*-terminal tail 77–110 might reflect the different

stability of the HLH fold; indeed, only in the former case the HLH domain was well-structured, whereas it was not well-defined in the latter case, as it was discussed above about the conformational properties of peptides **10** and **7**. This would imply a specific interaction pattern of the *N*-terminus with the folded HLH region, whereas the interaction would be mostly unspecific in the case of a partially unfolded HLH motif.

CONCLUSIONS

The Id2 protein is believed to be a promising target for tumor therapy, especially for neuroblastoma, where it has been shown to inhibit the function of pRb [16]. Therefore, both biochemical and conformational studies of Id2 are important to understand the mechanism of action and, later, to develop chemical tools to block the Id2–pRb interaction. Synthetic peptides derived from amino acid replacement and *N*-/*C*-end truncation of Id2 are useful to study the influence of different parts of the sequence on the structural properties of the protein. Here we have reported on a series of Id2 analogs with variable length, which were prepared by stepwise SPPS using Fmoc chemistry. The synthesis of the *C*-terminal region was found to be difficult and to strongly vary with the truncation point. More precisely, the *C*-end positions 124 and 110, but not 119, allowed the synthesis of large fragments. By excluding the chemical ligation approach for the synthesis of Id2 fragments containing the complete *C*-terminus due to the lack of native Cys residues in suitable positions, an alternative would be the condensation of fully protected fragments, which will be investigated by us in a future study.

Warburton and coworkers reported on the importance of Cys42 for Id2 homodimerization and function [30]. We also found that the HLH fold was sensitive to the substitution of its sulfur-containing residues as well as to the presence of *N*- and *C*-terminal extensions. On the basis of these results, fluorescent or ^{15}N-/^{13}C-labeled Id2 polypeptides will be designed for fluorescence-resonance-energy-transfer or NMR spectroscopy investigations to gain further insights into the folding behavior of the Id2 protein.

Acknowledgements

This work was supported by the Deutsche Forschungsgemeinschaft (Emmy-Noether grant no. CA296) and the Fonds der Chemischen Industrie.

REFERENCES

1. Perk J, Iavarone A, Benezra R. Id family of helix-loop-helix proteins in cancer. *Nat. Rev. Cancer* 2005; **5**: 603–614.
2. Yokota Y, Mori S. Role of Id family proteins in growth control. *J. Cell. Physiol.* 2002; **190**: 21–28.
3. Massari ME, Murre C. Helix-loop-helix proteins: regulators of transcription in eucaryotic organisms. *Mol. Cell. Biol.* 2000; **20**: 429–440.
4. Langlands K, Yin X, Anand G, Prochownik EV. Differential interactions of Id proteins with basic-helix-loop-helix transcription factors. *J. Biol. Chem.* 1997; **272**: 19785–19793.
5. Deed RW, Hara E, Atherton GT, Peters G, Norton JD. Regulation of Id3 cell cycle function by Cdk-2-dependent phosphorylation. *Mol. Cell. Biol.* 1997; **17**: 6815–6821.
6. Hara E, Hall M, Peters G. Cdk2-dependent phosphorylation of Id2 modulates activity of E2A-related transcription factors. *EMBO J.* 1997; **16**: 332–342.
7. Matsumura ME, Lobe DR, McNamara CA. Contribution of the helix-loop-helix factor Id2 to regulation of vascular smooth muscle cell proliferation. *J. Biol. Chem.* 2002; **277**: 7293–7297.
8. Fajerman I, Schwartz AL, Ciechanover A. Degradation of the Id2 developmental regulator: targeting via N-terminal ubiquitination. *Biochem. Biophys. Res. Commun.* 2004; **314**: 505–512.
9. Berse M, Bounpheng M, Huang X, Christy B, Pollmann C, Dubiel W. Ubiquitin-dependent degradation of Id1 and Id3 is mediated by the COP9 signalosome. *J. Mol. Biol.* 2004; **343**: 361–370.
10. Benezra R, Davis RL, Lockshon D, Turner DL, Weintraub H. The protein Id: a negative regulator of helix-loop-helix DNA binding proteins. *Cell* 1990; **61**: 49–59.
11. Norton JD. ID helix-loop-helix proteins in cell growth, differentiation and tumorigenesis. *J. Cell Sci.* 2000; **113**: 3897–3905.
12. Lasorella A, Uo T, Iavarone A. Id proteins at the cross-road of development and cancer. *Oncogene* 2001; **20**: 8326–8333.
13. Sikder HA, Devlin MK, Dunlap S, Ryu B, Alani RM. Id proteins in cell growth and tumorigenesis. *Cancer Cell* 2003; **3**: 525–530.
14. Iavarone A, Lasorella A. Id proteins in neural cancer. *Cancer Lett.* 2004; **204**: 189–196.
15. Vandeputte DA, Troost D, Leenstra S, Ijlst-Keizers H, Ramkema M, Bosch DA, Baas F, Das NK, Aronica E. Expression and distribution of id helix-loop-helix proteins in human astrocytic tumors. *Glia* 2002; **38**: 329–338.
16. Lasorella A, Noseda M, Beyna M, Yokota Y, Iavarone A. Id2 is a retinoblastoma protein target and mediates signalling by Myc oncoproteins. *Nature* 2000; **407**: 592–598.
17. Iavarone A, Garg P, Lasorella A, Hsu J, Israel MA. The helix-loop-helix protein Id-2 enhances cell proliferation and binds to the retinoblastoma protein. *Genes Dev.* 1994; **8**: 1270–1284.
18. Ohtani N, Zebedee Z, Huot TJ, Stinson JA, Sugimoto M, Ohashi Y, Sharrocks AD, Peters G, Hara E. Opposing effects of Ets and Id proteins on p16INK4a expression during cellular senescence. *Nature* 2001; **409**: 1067–1070.
19. Fong S, Debs RJ, Desprez PY. Id genes and proteins as promising targets in cancer therapy. *Trends Mol. Med.* 2004; **10**: 387–392.
20. Lasorella A, Boldrini R, Dominici C, Donfrancesco A, Yokota Y, Inserra A, Iavarone A. Id2 is critical for cellular proliferation and is the oncogenic effector of N-myc in human neuroblastoma. *Cancer Res.* 2002; **62**: 301–306.
21. Florio M, Hernandez MC, Yang H, Shu HK, Cleveland JL, Israel MA. Id2 promotes apoptosis by a novel mechanism independent of dimerization to basic helix-loop-helix factors. *Mol. Cell. Biol.* 1998; **18**: 5435–5444.
22. Mach H, Middaugh CR, Lewis RV. Statistical determination of the average values of the extinction coefficients of tryptophan and tyrosine in native proteins. *Anal. Biochem.* 1992; **200**: 74–80.
23. Whitmore L, Wallace BA. DICHROWEB, an online server for protein secondary structure analyses from circular dichroism spectroscopic data. *Nucleic Acids Res.* 2004; **32**: W668–W673.
24. Provencher SW, Glockner J. Estimation of globular protein secondary structure from circular dichroism. *Biochemistry* 1981; **20**: 33–37.

25. Chou PY, Fasman GD. Prediction of protein conformation. *Biochemistry* 1974; **13**: 222–245.
26. Abedini A, Raleigh DP. Incorporation of pseudoproline derivatives allows the facile synthesis of human IAPP, a highly amyloidogenic and aggregation-prone polypeptide. *Org. Lett.* 2005; **7**: 693–696.
27. Mutter M, Nefzi A, Sato T, Sun X, Wahl F, Wohr T. Pseudo-prolines (psi Pro) for accessing "inaccessible" peptides. *Pept. Res.* 1995; **8**: 145–153.
28. Kaiser E, Colescott RL, Bossinger CD, Cook PI. Color test for detection of free terminal amino groups in the solid-phase synthesis of peptides. *Anal. Biochem.* 1970; **34**: 595–598.
29. Kiewitz SD, Cabrele C. Synthesis and conformational properties of protein fragments based on the Id family of DNA-binding and cell-differentiation inhibitors. *Biopolymers (Pept. Sci.)* 2005; **80**: 762–774.
30. Liu J, Shi W, Warburton D. A cysteine residue in the helix-loop-helix domain of Id2 is critical for homodimerization and function. *Biochem. Biophys. Res. Commun.* 2000; **273**: 1042–1047.

